

Note to 8.13 students:

Feel free to look at this paper for some suggestions about the lab, but please reference/acknowledge me as if you had read my report or spoken to me in person. Also note that this is only one way to do the lab and data analysis, and there are nearly an infinite number of other things to do that would be better.

I made some mistakes doing this lab. Here are a couple I found (and some more tips):

- I did not account for the error from the distance measurement between the chopper wheel and the low efficacy detector
- The reactor temp is 50 C not 50 K

Neutron Physics

Rachel Bowens-Rubin*

MIT Department of Physics

(Dated: December 14, 2009)

Neutrons from uranium fission in the MIT nuclear reactor were used to determine the velocity distribution of neutrons in the reactor and measure the Bragg diffraction of neutrons scattering from a copper crystal. The velocity distribution of neutrons when measured close to their exit point resembled a convolution of two rectangles; the distribution far from the exit point was fit to a modified version of the Maxwell-Boltzmann distribution with inconclusive results. However, a linear fit of a semi-log plot of this data was more conclusive, and the temperature of the reactor was calculated to be $T = 75 \pm 110\text{K}$, which is within one standard deviation of the expected result. To measure Bragg diffraction, data were obtained at four different scattering angles. The velocities at these angles were found and plotted against their corresponding inverse-wavelength, predicted from the Bragg law. The linear fit of this plot yielded a value of $m_n/h = (4.02 \pm 0.39) \times 10^{-7} \text{ s/m}^2$.

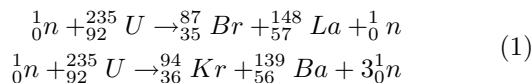
I. INTRODUCTION

In 1931, Walther Bothe and Herbert Becker discovered a strange radiation which was proven to be from neutrons. Before the turn of 1940, it was discovered that neutrons could react with uranium to produce new neutrons, lighter elements, and abundant amounts of energy. New technologies utilizing neutron-uranium reactions began to develop including nuclear reactors and atomic bombs which are still used today. To fully understand these technologies, it is important to know how neutrons behave and their properties in thermal equilibrium. ^[1]

II. THEORY

A. Neutron Production in a Nuclear Reactor

Inside the core of a nuclear reactor, neutrons traveling at a slow velocity react with U-235 to create lighter elements and neutrons traveling at faster velocities (Equation 1). The mass lost in these reactions contributes to the kinetic energy of the reaction fragments.



In order to sustain the reactions in the core, the fast velocity neutrons must be slowed in order to react with more U-235. The neutrons are slowed by scattering off a moderator material made of light atoms (water is used in the reactor at MIT). Each scatter reduces the neutron's kinetic energy until it is at the mean energy of the moderator atoms and is in thermal equilibrium. The moderator is controlled such that the thermal equilibrium temperature corresponds to an energy at which the neutrons are

slow enough to react with the U-235.

B. Maxwell-Boltzmann Distribution

Because neutrons inside the reactor share the properties of an ideal gas in thermal equilibrium that does not experience quantum or relativistic effects, their velocity distribution can be described by the Maxwell-Boltzmann relationship,

$$n(v)dv = \frac{4N}{\sqrt{\pi}} \left(\frac{v^2}{v_0^3} \right) \exp\left(-\frac{v^2}{v_0^2} \right) dv \quad (2)$$

where v is the velocity of the neutrons, v_0 is the most probable velocity of the neutrons, N is the volume density of the neutrons in the reactor, and $n(v)dv$ is the density of the neutrons with velocity between v and $v + dv$. The relationships for an ideal gas between energy, mass, velocity, and temperature also apply.

C. Bragg Diffraction

In 1924, Louis De Broglie suggested that all matter has a wavelength (λ) which depends on its momentum (mv) according to the relationship

$$\lambda = \frac{h}{mv} \quad (3)$$

where h is Planck's constant. Because a neutron has a small mass, it will have a small momentum and thus a measurable wavelength. The wavelike properties of neutrons are evident when they are scattered off atoms in a crystal, because they obey Bragg's law for the scattering of radiation,

$$n\lambda = 2d\sin(\theta_B) \quad (4)$$

*Electronic address: rbowru@mit.edu

where n is the diffraction order, λ is the wavelength, d is the interplanar spacing in the crystal, and θ_B is the Bragg angle. The Bragg angle is the angle between the incident and reflected ray (shown in Figure 1).

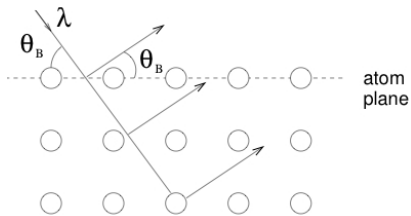


FIG. 1: The incoming wave (with wavelength λ and incoming angle θ_B) scatters off a crystal with an outgoing angle also equal to θ_B .^[1]

III. EXPERIMENTAL SETUP

A. Apparatus

To measure different properties of neutrons, an apparatus located in the MIT reactor (building NW12) was used to collect data. The counts of the incoming neutrons versus the time at which they reached a detector were measured in time bins called channel numbers. The measurements were displayed in a program called *Lab-View*. The setup could be run remotely through *iLab*, but the connection was often unreliable, which often caused difficulties in data collection.

The neutrons traveled through an opening in the reactor shielding and exited through a rectangular slit. From the slit the neutrons traveled and encountered a spinning cadmium chopper wheel with eight openings about a millimeter wide. The spinning chopper wheel absorbed the neutrons which hit the wheel when it was blocking the neutrons path, but allowed neutrons to pass if they managed to reach the wheel when one of the openings was in its path (left image in Figure 2).

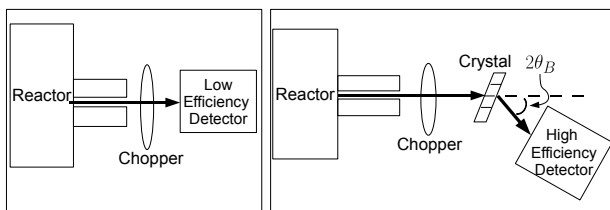


FIG. 2: (Left) The experimental setup for measuring the time of flight. (Right) The experimental setup for measuring Bragg diffraction.

To study the velocity distribution of neutrons emerging from the reactor, a low efficiency detector made of BF_3 gas was placed in the pathway of the beam (this setup

is shown in the left image in Figure 2). Because the interaction between boron and neutrons depends on the inverse of the neutron's velocity, the efficiency of the detector was proportional to $1/v$. The detector was aligned in the transverse direction by running a scan to find the placement with the maximum measured intensity.

For the Bragg diffraction experiment, the low efficiency detector was removed from the path of the neutrons and a copper crystal, which could be rotated to measure different Bragg angles, was moved into the beam path. The crystal scattered the neutrons at twice the Bragg angle toward the high efficiency detector, which could be rotated to intercept the beam when the crystal was at different rotations. The high efficiency detector was aligned at each crystal rotation by performing an angle scan to find a point in which the intensity was a maximum. An example of the angle scan at 30° is shown in the right image in Figure 3.

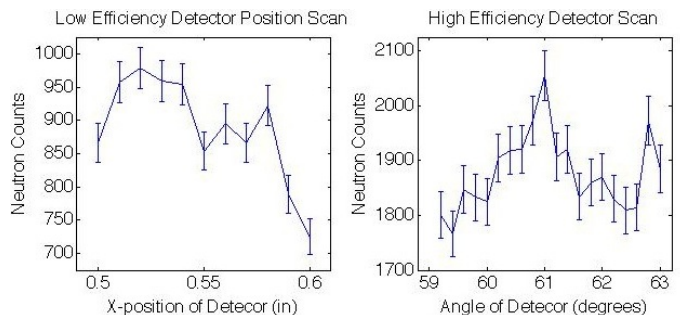


FIG. 3: (Left) Low efficiency detector transverse direction placement scan at the near time-of-flight position. (Right) High efficiency detector angle placement scan for $\theta_B = 30^\circ$.

IV. RESULTS AND DISCUSSION

A. Time of Flight

Time-of-flight spectroscopy was performed with the low efficiency detector at three different distances away from the chopper wheel. For the near scan, the low efficiency detector was located 8.255cm away from the chopper wheel, and the time was measured using $2\mu\text{s}$ time bins with 1000 channels. Because the neutrons traveling at different velocities do not have much distance to separate, the distribution of the near scan was described by the convolution of the rectangular slit from the opening in the shielding and the rectangular slit in the chopper wheel (Figure 4). Thus the data from the near scan was fit to a triangular distribution producing a reduced chi square of $\chi_{red}^2=1.01$. The results of the near scan were also used to calculate the value of the total intensity of the neutrons coming out of the reactor $I = 145 \pm 13$ counts/s.

For the midrange scan, the detector was located 50.80cm away from the chopper wheel, and the time was

measured using $4\mu\text{s}$ time bins with 500 channels. At this distance, the velocity distribution widens and becomes a convolution of the triangular and the Maxwell-Boltzmann distributions. (Figure 4).

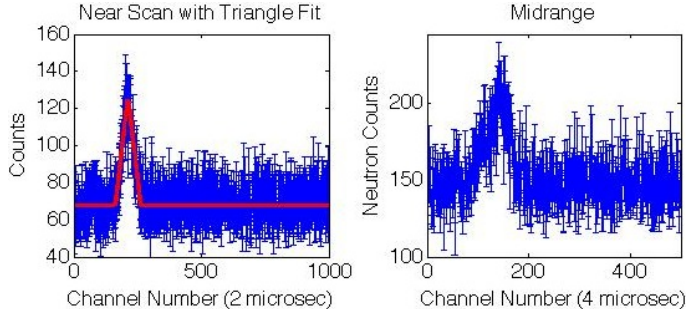


FIG. 4: (left) Near data with Triangle Fit (Counts versus Channel Number). (right) Raw Midrange Data (Counts versus Channel Number).

For the far scan, the low efficiency detector was located at 1.27m away from the chopper wheel, and time was measured using $2\mu\text{s}$ time bins with 1000 channels (Figure 5). By this distance, the number of neutrons at each velocity was wider than the midrange scan. In the lower channel numbers, there is a spike from the faster neutrons, while the higher channel numbers show a distribution from the slower neutrons. The slower neutron data (channel numbers 300 to 1000) were fitted to a version of the Maxwell-Boltzmann distribution that was corrected for the efficiency of the detector:

$$j'(v)dv = Bv^2 \exp\left(-\frac{v^2}{v_0^2}\right) dv \quad (5)$$

where v is the neutron velocity, v_0 is the most probable velocity, B is a proportionality constant, and $j'(v)dv$ is the detected density for neutrons between speeds v and dv . This fit predicted the most probable velocity to be $v_0 = 3135 \pm 75$ m/s and has a reduced chi square of $\chi_{red}^2 = 1.18$.

As a test, a triangle distribution was also fit to the far data. Surprisingly this fit produced a reduced chi square of $\chi_{red}^2 = 1.14$ which was closer to one than the Maxwell-Boltzmann distribution. This is an indication that v_0 cannot conclusively be determined by the modified Maxwell-Boltzmann fit.

Using another method to obtain a different value for v_0 , a linear fit was made of the plot of $\ln(N_i/v_i^4)$ versus v_i^2 to find a slope value equal to $1/v_0^2$ (these relationships are derived from Equation 5). High velocity neutrons were not included in the fit because their measured time-of-flight differed from their true time-of-flight because they continued to lose a noticeable portion of their velocity as they travel toward the detector and their interaction with chopper wheel distorts their velocity distribution. Low velocity neutrons were also not included

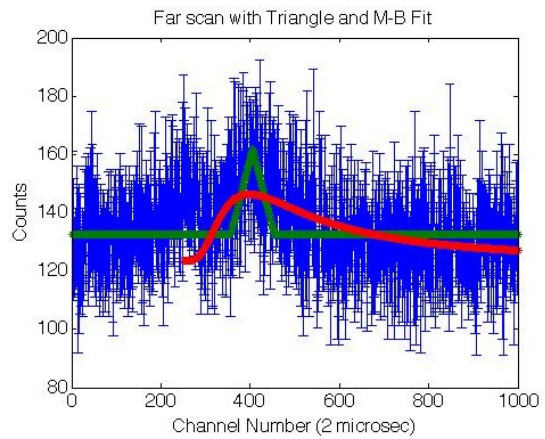


FIG. 5: Far Scan with Fits (Channel Number versus Counts). The red line is a fit of the data to the Maxwell-Boltzmann distribution, taking into account the efficiency of the detector, which had a reduced chi square of $\chi_{red}^2=1.18$. The green line represents a triangle fit to the data, which had a reduced chi square of $\chi_{red}^2=1.14$

because their counts could not be distinguished from the background noise. The points included in this fit were those which accounted for ten percent of the total intensity, centered around the most probable velocity as calculated from the initial fit from the modified Maxwell-Boltzmann distribution (see above). This corresponded to the channel numbers ranging from 382 to 414. This method produced a new value for the most probable velocity of $v_0 = 1105 \pm 813$ m/s which corresponds to a temperature inside the reactor of $T = 75 \pm 110$ K. This temperature is within one standard deviation of the expected value of $T = 50$ K.

The results of the near and far scans were also used to calculate the channel offset of $n_0 = 199 \pm 5.7$ for time bins of $2\mu\text{s}$. The channel offset is the number of time bins that pass between when the low efficiency detector gets a signal from the “slit detector” to start recording and when the neutrons start to pass through the opening in the chopper wheel. The value for the channel offset is used next in the calculation of the velocity distribution of the Bragg angles.

B. Bragg Diffraction

Time-of-flight spectroscopy was performed using the setup for Bragg diffraction with the high efficiency detector. In collaboration with Sean Westerdale and Anna Waldman-Brown, scans were obtained with the crystal rotated such that neutrons scattered from the (002) plane at four different angles of $\theta_B = 15^\circ, 20^\circ, 25^\circ$, and 30° ; two scans were obtained for $\theta_B = 20^\circ$. Each scan was formatted to contain 500 channel numbers with each channel number representing a $4\mu\text{s}$ time bin. The channel number (m) was converted into velocity(v) by

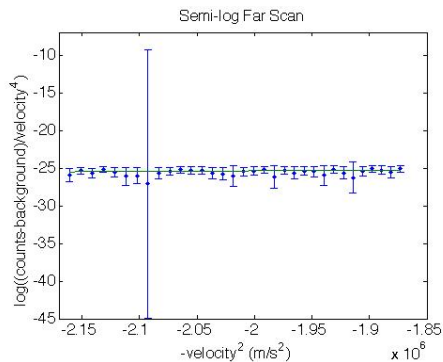


FIG. 6: Semi-log Fit of Far Data. A linearized version of the modified Maxwell-Boltzmann distribution was fitted to obtain a value of $v_0 = 1105 \pm 813$ m/s.

$$v = \frac{L}{t_d(m - n_0)} \quad (6)$$

where L is the distance the neutron travels between the chopper wheel and the high efficiency detector, t_d is the bin time ($4\mu\text{s}$), and n_0 is the channel offset calculated from the near and far time of flight data.

Because the crystal scatters neutrons of one particular velocity at the angle of the high efficiency detector, the only distribution of the velocities was from the convolution of the rectangular openings from the chopper and shielding, so a triangular distribution was measured. The peak of the triangle fit corresponded to the measured velocity at that crystal rotation. Figure 7 shows one of the scans taken using $\theta_B = 20^\circ$. A fit was obtained for every scan except $\theta_B = 15^\circ$ because the peak was indistinguishable from the background counts.

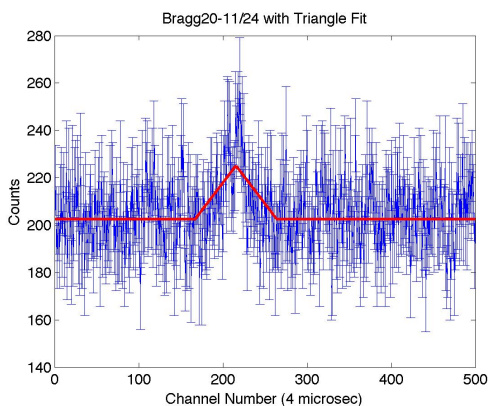


FIG. 7: Bragg diffraction at $\theta_B = 20^\circ$ (counts versus channel number). This scan was taken on November 24th and took about three hours to run. The data were fit to a triangular distribution and the peak was taken to correspond to the velocity of the neutrons scattered at $\theta_B = 20^\circ$.

A correction to the Bragg angle was applied using the

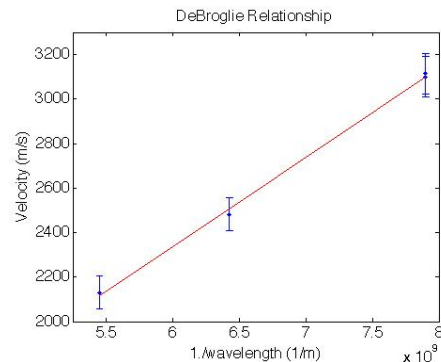


FIG. 8: DeBroglie Relationship ($1/\lambda$ versus velocity). The DeBroglie relationship was plotted to find a value for $m_n/h = (4.02 \pm 0.39 \times 10^{-7} \text{ s/m}^2)$

measured maximum intensity point found in the high efficiency detector alignment. The Bragg angle was assigned to be one-half of the angle which the high efficiency detector measured the largest intensity. This angle was then used to calculate the expected wavelength using the Bragg law (Equation 4).

Once the neutron velocity and expected wavelength for each angle were found, a plot of $1/\lambda$ against the velocity (Equation 3) was made and fitted linearly to obtain a slope value equal to $m_n/h = (4.02 \pm 0.39) \times 10^{-7} \text{ s/m}^2$ (Figure 8). This is within one standard deviation of the expected value $h/m_n = 3.96 \times 10^{-7} \text{ s/m}^2$.

V. SUMMARY

The velocity distribution of neutrons inside the MIT nuclear reactor was studied by measuring the time-of-flight of neutrons traveling between a chopper wheel, which creates a concentrated beam of neutrons, and a low efficiency detector. When the low efficiency detector was close to the chopper wheel, the velocity distribution was described by a convolution between the rectangular openings in the chopper wheel and shielding. At greater distances a modified version of the Maxwell-Boltzmann distribution, which accounted for the efficiency of the detector, and a triangle distribution, which returned a . A semi-log plot was also made to calculate $v_0 = 1105 \pm 813$ m/s, which corresponds to a temperature of $T = 75 \pm 110$ K which is within one standard deviation of the expected value (50 K).

Bragg scattering of neutrons was also studied using a copper crystal and a high efficiency detector. Scans were taken with the crystal the four different angles of around $\theta_B = 15^\circ, 20^\circ, 25^\circ$ and 30° , and a triangular distribution was fit successfully to three of these angles. The exact values of the Bragg angles were found by finding the angle where the high efficiency detector measured the most counts, and using the Bragg law, the predicted wavelength was calculated from the found corrected Bragg angle. A linear fit derived from the DeBroglie relationship

was then made to find $m_n/h = (4.02 \pm 0.39) \times 10^{-7} \text{s/m}^2$, which is within one standard deviation of the expected value of $h/m_n = 3.96 \times 10^{-7} \text{s/m}^2$.

scan and the 20° and 30° scattering angles, Kathryn Decker French for taking data with me and only lighting me on fire once this semester, and Sid Creutz for proof reading my paper.

Acknowledgments

I would like to acknowledge Sean Westerdale and Anna Waldman-Brown for sharing their data for the midrange

[1] MIT Physics Department, *Junior lab written report notes* (August, 2005).